SCIENTIFIC REPORTS

OPEN

SUBJECT AREAS:
SUB-WAVELENGTH OPTICS
NANOPHOTONICS AND PLASMONICS
ADAPTIVE OPTICS
PHOTONIC DEVICES

Received
18 April 2013

Accepted
18 April 2013

Published
9 May 2013

Correspondence and requests for materials should be addressed to M.M. (michael.mazilu@st-andrews.ac.uk)

* These authors contributed equally to this work.

Coherent control of plasmonic nanoantennas using optical eigenmodes

Sebastian Kosmeier[1]*, Anna Chiara De Luca[1,2]*, Svetlana Zolotovskaya[1], Andrea Di Falco[1], Kishan Dholakia[1] & Michael Mazilu[1]

[1]SUPA, School of Physics and Astronomy, University of St Andrews, North Haugh, KY16 9SS, St Andrews, UK, [2]Institute of Protein Biochemistry, National Research Council, Via P. Castellino 111, 80313, Naples, Italy.

The last decade has seen subwavelength focusing of the electromagnetic field in the proximity of nanoplasmonic structures with various designs. However, a shared issue is the spatial confinement of the field, which is mostly inflexible and limited to fixed locations determined by the geometry of the nanostructures, which hampers many applications. Here, we coherently address numerically and experimentally single and multiple plasmonic nanostructures chosen from a given array, resorting to the principle of optical eigenmodes. By decomposing the light field into optical eigenmodes, specifically tailored to the nanostructure, we create a subwavelength, selective and dynamic control of the incident light. The coherent control of plasmonic nanoantennas using this approach shows an almost zero crosstalk. This approach is applicable even in the presence of large transmission aberrations, such as present in holographic diffusers and multimode fibres. The method presents a paradigm shift for the addressing of plasmonic nanostructures by light.

Accurate and dynamic coherent control of the optical near-field at the subwavelength scale is a newly emerging topic in nanoscience. The subwavelength concentration of the electromagnetic field can be achieved in the proximity of plasmonic nanostructures such as nanoantennas, nanopads or sharp tips due to the strong surface charge gradients present in such devices. The confinement and manipulation of light energy from a laser source to a single molecular target plays a key role in the miniaturization of optical devices with important applications in the fields of optical trapping[1–4] and sensing based on fluorescence or surface enhanced Raman spectroscopy[5–8]. The spatially selective field enhancement is largely dictated by the geometry of the metal system, which for fixed patterns and standard plane wave illumination is inflexible. Beyond confining light at fixed locations (hotspots) there is a burgeoning need for the dynamic control of the light field that would allow a facile method to create the optical near-field of choice and obviate issues of crosstalk between adjacent nanostructures in a given array.

Different approaches have recently been proposed to reach coherent control in plasmonic structures[9–15]. Stockman et al.[9] proposed using temporal phase and amplitude shaping of ultrashort laser pulses to illuminate random plasmonic nanostructures. The experimental implementation of this idea, based on the combination of pulse shaping with a learning algorithm, has been demonstrated by Aeschlimann and coworkers[11]. Another approach of coherent control is to fabricate periodical arrays of nanostructures and then selectively excite specific array elements by spatially shaping the incident light field[16], e.g. into higher order transverse Hermite-Gaussian (HG) modes[12]. Volpe and colleagues also proposed a deterministic optical inversion (DOPTI) algorithm taking the desired near-field distribution and establishing a physical solution for the incident field, expressed as a superposition of HG beams[17]. However, the proximity between the elements on a high density array of nanodevices renders a precise addressing, without crosstalk, of a single device very challenging. Indeed, it is important to establish an exact mathematical formalism that treats the plasmonic-optical system in unison so that we can ensure the incident field is pertinent to achieve a given near-field without exciting other nanodevices. The purpose of the present manuscript is to determine the optimal solution of this problem.

Our approach to overcome the crosstalk limitation is through the decomposition of the light field on an array of nanoelements into optical eigenmodes (OEi)[18]. This decomposition offers a system dependent orthogonal representation of the optical fields and can be used to achieve optimal optical sorting of nano-particles[19], sub-diffractive imaging[20], optimal sub-wavelength focusing[21] and compressive imaging[18]. Here, we use this decomposition in an original application to suppress the crosstalk between the plasmonic hotspots in the device considered. We demonstrate the power and versatility of the approach with two methods that use the OEi for

the selective structured illumination of an array of nanoantennas and nanopads. Both of our approaches feature an automatic (inherent) aberration correction, and one leads to the reduction of crosstalk observed. This OEi approach supersedes all previous studies and we contend is the method of choice of addressing metallic nanostructures for applications including optical micromanipulation, sensing, spectroscopy and near-field imaging.

Results

Optical eigenmodes for selective illumination of nanoantennas. We firstly describe the method in terms of the structured illumination of an array of p nanoantennas able to create an intensity hotspot (see Fig. 1a) in the gap between the nanoantenna arms. With each hotspot we associate a region of interest R_i where the index i indicates the nanoantenna number. By generalising the OEi method[18], we define a multi-region intensity operator valid across the whole array. To define this operator, we consider the incident electromagnetic field E as composed of a superposition of N monochromatic (E_j) scalar "probe" fields

$$E = \sum_{j=1}^{N} a_j^* E_j \tag{1}$$

where a_j are the complex amplitude coefficients of the fields E_j. The number of probe fields N considered need to be chosen such as to cover the optical degrees of freedom available in the optical system[22,18]. The total intensity $m(E)$ integrated over the multiple regions (R_i) of the array is defined by:

$$m(E) = \sum_{i=1}^{p} \int_{R_i} EE^* \, d\sigma. \tag{2}$$

This allows us to define a set of field orthogonal illuminations $\mathbb{E}_\ell$ with respect to the total intensity called optical eigenmodes (see supplementary information for details). These optical eigenmodes are ordered with respect to their eigenvalues λ_ℓ and the eigenmode with the largest eigenvalue $\lambda_{\ell=1}$ describes the superposition of initial fields E_j delivering the maximum total intensity[23] across the multiple regions of interest R_i. Further, considering a single region of interest would correspond to the structured illumination having the maximal coupling to the associated hotspot. This approach corresponds to the *first method*, discussed in this paper, to highlight a specific hotspot (see Fig. 1b).

As a *second method*, we can define a p-dimensional complex vector corresponding to a target illumination field P_j where each element corresponds to the amplitude and phase of a constant electric field in the region of interest R_i. This target field can be decomposed onto the optical eigenmode base using a projection defined by:

$$c_\ell = \sum_{i=1}^{p} \int_{R_i} P^* \mathbb{E}_\ell \, d\sigma \tag{3}$$

where c_ℓ corresponds to the complex decomposition coefficients of the field P in base $\mathbb{E}_\ell$. If the $\mathbb{E}_\ell$ fields form a complete base, we can perfectly reconstruct the unknown field P from the projection using $P = \sum_\ell c_\ell \mathbb{E}_\ell$. We remark that the completeness of the base is dependent on the initial fields probing all the optical degrees of freedom available i.e. the order at which we stop the probing when using the Hermite-Gaussian beams, for example. Using this *second method*, we can highlight multiple hotspots *simultaneously*, while addressing the remaining nanostructures with darkness, hence avoiding crosstalk (see Fig. 1c).

Each of the two possible methods, single hotspot illumination and target field decomposition, describe the coupling to individual hotspots defined by the array of nanoantennas. The *first method* delivers the highest coupling efficiency regardless of crosstalk between different hotspots. The *second method* delivers the smallest possible

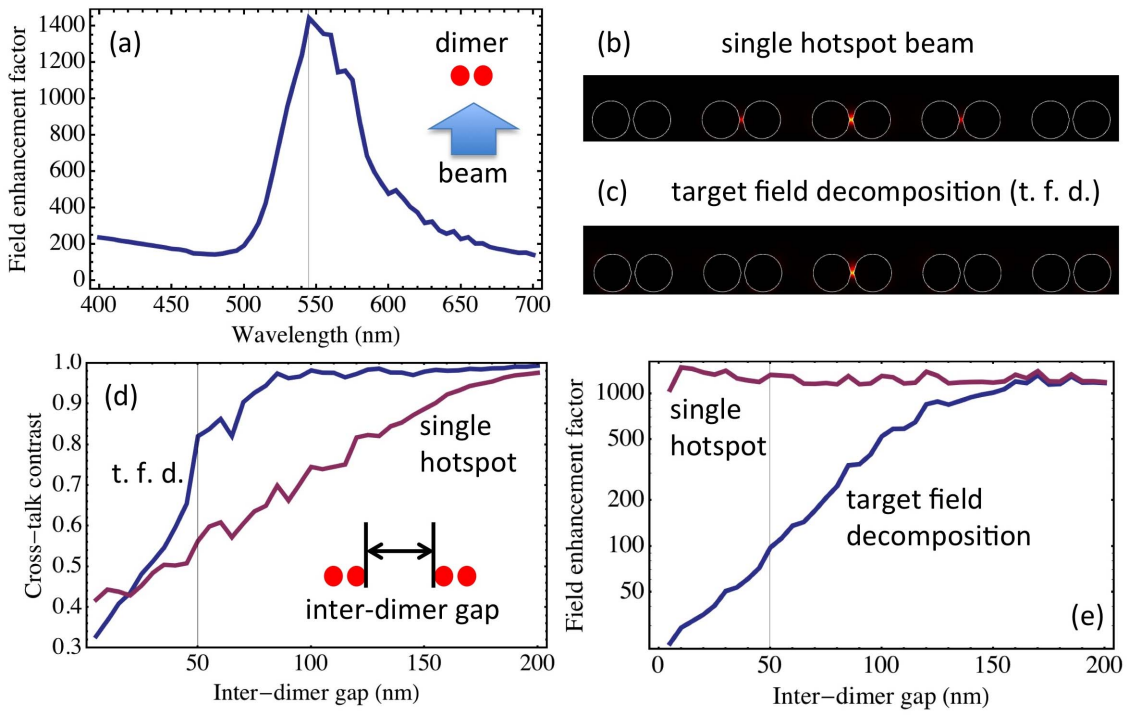

Figure 1 | Hotspot illumination of gold nanoparticle dimers (particle size 60 nm and dimer gap 5 nm). (a) Spectral response of the field enhancement factor under plane wave illumination. The enhancement factor is defined as the ratio of the field in the center of the dimer to the field, in the same position, in the absence of the dimer. All remaining figures are at the resonant wavelength of 545 nm. (b, c) Electric field intensity when illuminating a chain of 5 dimers (inter-dimer gap 50 nm) with (b) a focused beam and (c) the target field decomposition. (d) Crosstalk contrast between the targeted hotspot and surrounding hotspots for (red) the single hotspot beam and for (blue) the target field decomposition. (e) Field enhancement factor in the highlighted hotspot for (red) the single hotspot beam and for (blue) the target field decomposition.

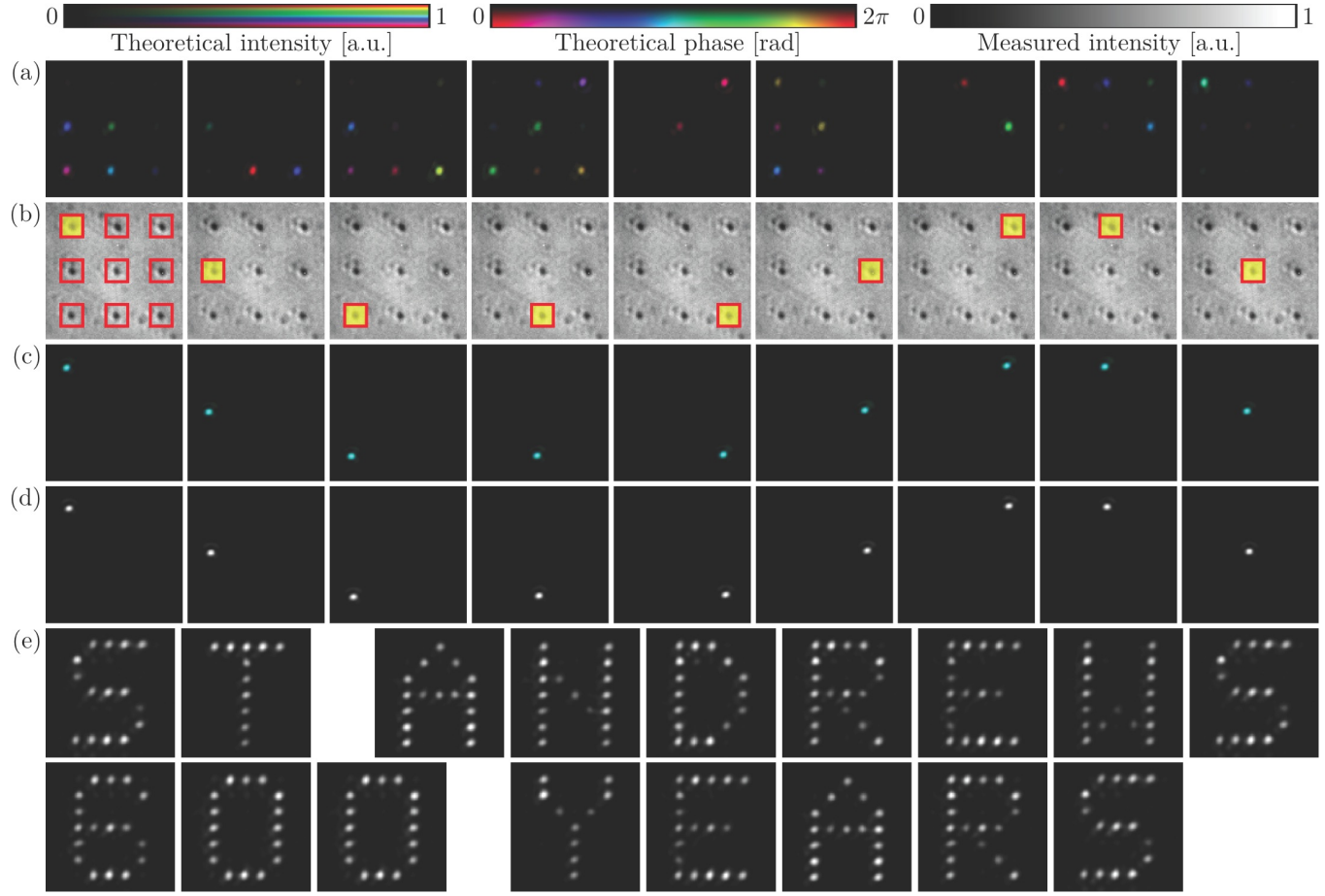

Figure 2 | (a) The 3 × 3 experimentally determined optical eigenmodes color-coded depending on phase and amplitude. (b) The 3 × 3 hotspot region of interest (red squares) together with the highlighting target field (yellow). (c–d) Predicted and experimental single nanoantennas highlighting beams (*first method*). (e) Selective illumination of a 7 × 7 array of nanopads celebrating 600 years of the University of St. Andrews (*second method*).

crosstalk and highest "mode purity". We remark that, fundamentally, zero crosstalk can only be achieved when the optical degrees of freedom[22] of the optical system are larger or equal then the number of hotspots, showing a physical limit of this linear approach. Additionally, the target field decomposition allows for the coherent phase and amplitude addressing of the nanoantennas. This property is also maintained, to some extent, when the high nanostructure density implies crosstalk (see Fig. 1d, e).

The experimental setup consists of a first order diffracting spatial light modulator (SLM) that is used as a phase and amplitude filter to generate computer controlled structured illumination. We illuminate the sample with a coherent laser beam at 785 nm. In our experiment, we used $N = 164$ probe beams to determine the intensity Optical Eigenmodes ($\mathbb{E}_\ell$) in the CCD camera plane imaging the nanoantenna array using the approach outlined in the experimental method section. The illumination probes used are a theoretically predetermined orthogonal set of beams to guarantee a very efficient probing (see supplementary information for more details). In a first step, we use an area consisting of 9 antennas, implying that only 9 out of the 164 eigenmodes have non-zero eigenvalues (these 9 eigenmodes are illustrated in Fig. 2-a). Using these experimentally determined OEi, we can controllably highlight different hotspot regions (Fig. 2-b) using the target field decomposition method defined by eq. (3). The highlighting results can be predicted using the superposition relationship $\mathrm{P} = \sum_\ell c_\ell \mathbb{E}_\ell$ (see Fig. 2-c) and experimentally verified by displaying on the SLM the masks associated with the superposition of the OEi (see Fig. 2-d). To demonstrate the capability of our approach, we increase the number of degrees of freedom, i.e. addressable nanoelements, on the sample and complexity of the highlighting target. More

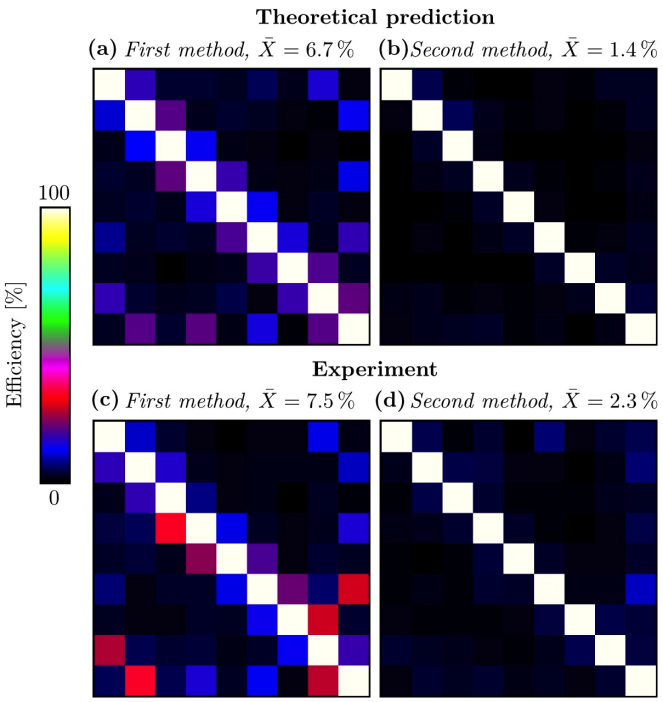

Figure 3 | (a, c) Crosstalk matrix for selective single spot illumination (*first method*) of a 3 × 3 array of nanopads with (a) prediction and (c) experimental measure. (b, d) Crosstalk matrix for target field decomposition (*second method*).

specifically, the plasmonic sample used is a periodical square array of 7×7 nanopads with a diameter of 330 nm and a period of 800 nm comparable to the laser wavelength. Figure 2-e shows the results from encoding the letters and numbers for a "St Andrews 600 Years" celebration banner.

Crosstalk characterisation. To quantify the overall coupling efficiency, we predict and measure the crosstalk matrix consisting of the intensities in the different hotspots while highlighting only one of them. For this, we select a 3×3 subset from the nanopads array and restrict the accessible numerical aperture (NA) of the microscope objective to about 0.4. This ensures that the diffraction limited Gaussian beam cannot illuminate a single nanopad without partly illuminating its neighbours, hence creating illumination crosstalk. That crosstalk is illustrated in Fig. 3 in terms of crosstalk matrices. Each column of a matrix corresponds to the addressing of another of the 9 nanopads and the elements of each column represent the intensity on each nanopad normalised to the response of the addressed pad. Thus a perfect selective coherent control case would result in a pure diagonal matrix. In a first instance, a single nanopad is illuminated using the single spot illumination (*first method*, Fig. 3-a, c) and in a second instance the target field decomposition (*second method*, Fig. 3-b, d) is used. The average crosstalk $\bar{X}$ on the 3×3 array is defined by the sum of all the off-diagonal matrix elements normalised to the sum of all the diagonal elements. A zero crosstalk corresponds to perfectly selective coherent control. *First method:* In this method, the sample is probed with the test fields E_j and we determine the first OEi $\mathbb{E}_1$ with respect to the specific nanopad that is addressed. This first eigenmode $\mathbb{E}_1$ maximises the intensity on the addressed nanopad, hence this illumination delivers almost identical results to a focussed Gaussian beam. The only advantage is the automatic aberration correction delivered by the experimental probing on the optical system. *Second method:* Here, the OEis are calculated with respect to all 3×3 nanopads and not just one. As these OEi are orthogonal, their superposition can reconstruct a field that highlights a single nanopad while leaving the other nanopads in the dark. In Fig. 3, we observe that for both methods the diagonal terms are the most important ones. However, the *first method* is accompanied by a few percent crosstalk while the *second method* shows 70% reduced crosstalk.

The suppressed crosstalk behaviour achieved using target field decomposition is also observable when considering plasmonic nanopads with much smaller periodicity. We have carried out the same experiments with a sample of 200 nm nanopads spaced with a period of 400 nm, where we restricted the illumination NA to approximately 0.8 on the SLM implying a clear crosstalk for a focussed beam. Reducing even further the NA does not deliver the necessary optical degrees of freedom to achieve crosstalk free selective illumination. In this case, we experimentally observed an average crosstalk reduction of 55% comparing the target field decomposition to the single hotspot eigenmode. As for the 800 nm spaced nanopads, the experimental results are in reasonable agreement with the predictions.

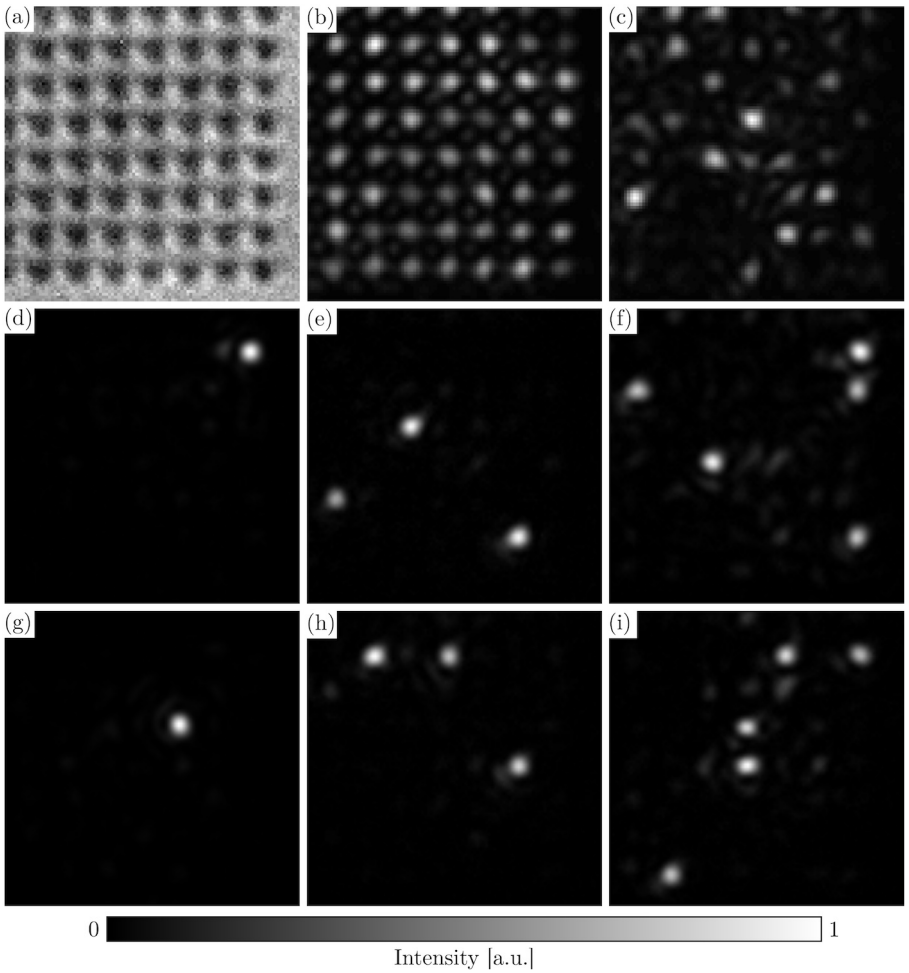

Figure 4 | (a) Whitelight image of the 7×7 array of 300 nm nanopads spaced with a period of 800 nm. Illumination of this array with (b) the reference beam without diffuser and (c) with the diffuser distorting the wavefront. Illumination using the eigenmode target field (*second method*) decomposition method of (d, g) one randomly selected nanopad, (e, h) three and (f, i) five randomly selected nanopads.

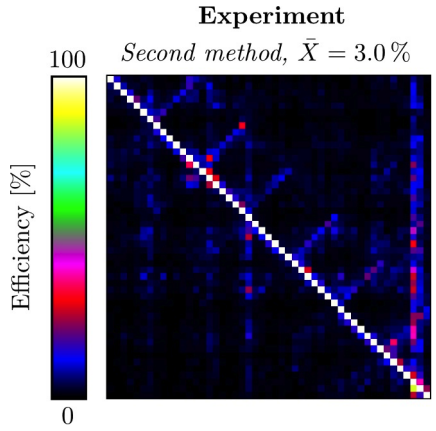

Figure 5 | Experimental crosstalk matrix for target field decomposition of a 7 × 7 array of nanopads in presence of the holographic diffuser.

Crosstalk characterisation in presence of diffuser. We additionally measured orthogonal eigenmodes for the illuminating laser light propagating through an optical diffuser. In this case, a holographic diffuser (1° diffusing angle, Edmund Optics) is positioned 1 cm after the iris (see the experimental set-up in the supplementary information). The diffused laser light is used to illuminate the same 7 × 7 nanopads array as in Fig. 2-e. In absence of the diffuser, the sample is almost uniformly illuminated by a reference beam (see Fig. 4-b), while in presence of the holographic diffuser, the illumination is heavily distorted, as shown in Fig. 4-c. In this illumination condition, a controlled addressing of individual antennas is clearly impossible. After experimentally determining the OEi of the 7 × 7 hotspots with the diffuser in place, we can properly address any single or multiple nanopads as demonstrated in Fig. 4-(d–i). The focusing onto one nanopad is illustrated in Fig. 4-(d, g) and the resulting low crosstalk even with the strong aberrations is visualised in Fig. 5. The simultaneous addressing of three (Fig. 4-(e, h)) or five (Fig. 4-(f, i)) randomly chosen independent nanopads underlines the automatic full field wavefront correction of the OEi approach. However, we observe an increased crosstalk when increasing the number of addressed nanopads (see Fig. 5) probably linked to the number of optical degrees of freedom[22].

The possibility to apply the selective highlighting after transmission through highly diffusive materials is an important advantage for biomedical sensing, imaging applications and fibre based technology in imaging, manipulation and nanosurgery. We have implemented a proof of principle application where we use a multimode optical fibre for the coherent light delivery to an array of plasmonic nanopads. After probing the optical system including the fibre, the OEi fields are then used for selective highlighting of a 2 × 2 nanopad array implementing the target field decomposition method. The experimental results of illumination of one and two randomly chosen nanopads are shown in Fig. 6. It should be noted that the selective highlighting of single and multiple nanoelements at different locations with the multimode fibre illumination does not require additional probing as aberration correction is inherent to the OEi.

Discussion

We have demonstrated a robust method, based on the OEi decomposition of light, to selectively address single or multiple elements chosen from an array of plasmonic nanostructures. More precisely, Figure 2 depicts the selective illumination of a 7 × 7 array of nanopads celebrating 600 years of the University of St. Andrews. Altogether, these results show that the OEi decomposition provides selective highlighting and the light is indeed directed exactly onto the intended nanostructures, hence demonstrating the basic functionality of OEi based optical coherent control.

The method reduces the crosstalk between the different plasmonic devices and is applicable even in the presence of large transmission aberrations. In fact, in Figure 3, we observe that for both methods the diagonal terms are the most important ones. However, the *first method* is accompanied by a few percent crosstalk while the *second method* shows 70% reduced crosstalk. The experimental results are in good agreement with the predictions and can be understood by considering that the target field decomposition ensures the highest possible "mode purity" at the expense of overall coupling efficiency while the single hotspot eigenmode ensures highest possible coupling efficiency at the expense of "mode purity".

The experimental probing procedure that we have implemented to determine the OEi has a second benefit. It automatically takes into account any time stationary optical imperfection and aberration for the given optical-plasmonic system. This means that measured orthogonal eigenmodes can even be determined for the illuminating laser light propagating through an optical diffuser, as shown in Fig. 4. These results demonstrate the flexibility of the OEi method for active independent multiplexing even in presence of large aberrations. Especially, this latter feature makes the approach highly promising for biomedical applications involving scattering cells and tissues. The method is general and does not rely on the periodicity of the utilised nanostructures. Hence, it can equally be used to highlight irregular arrays of devices.

Further, this approach can be extended to highlight different parts of more complex nanopatterns provided the optical system can access enough optical degrees of freedom. The probing and OEi approach can also be employed beyond the simple selective

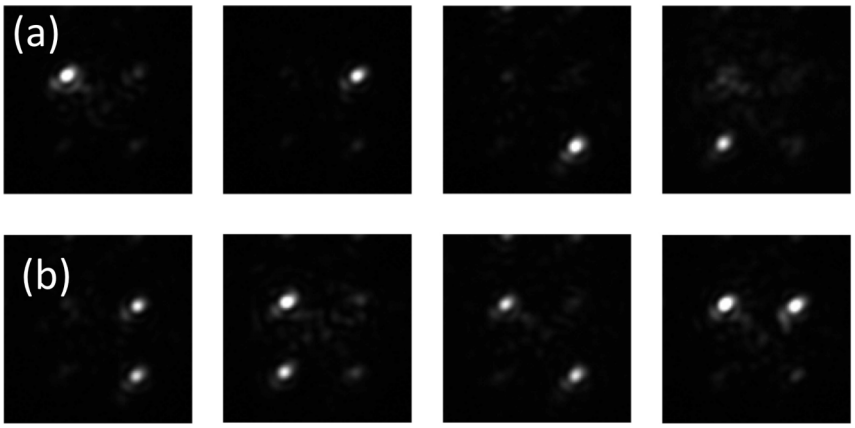

Figure 6 | Selective highlighting of one (a) and two (b) randomly chosen nanopads of a 2 × 2 nanopad array (*second method*).

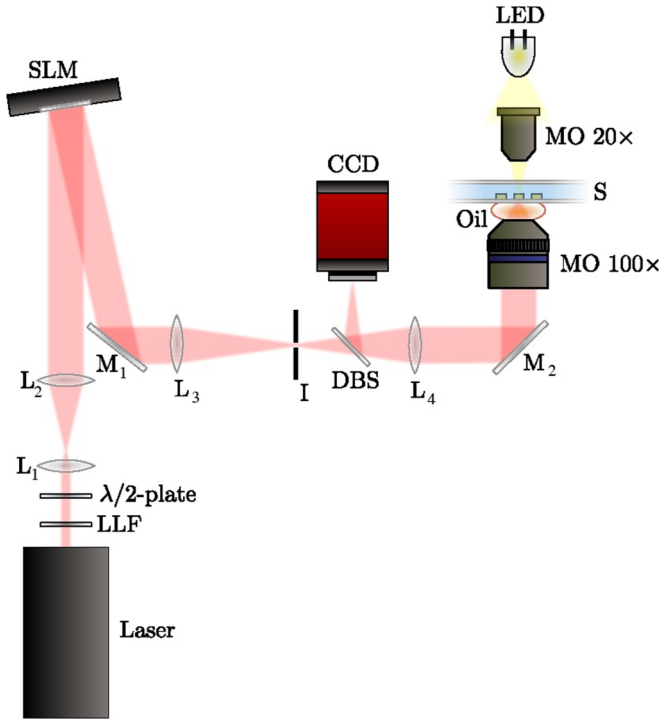

Figure 7 | Experimental setup for optical eigenmode based coherent control. Abbreviations: LLF: Laser line filter at 785 nm; L_i: Lenses; SLM: Spatial light modulator; M_i: Mirrors; I: Iris to filter out first diffraction order of the SLM; DBS: Dichroic beam splitter reflecting visible light and transmitting infrared light; CCD: CCD camera; MO: Microscope objective; S: Sample.

highlighting. Indeed, the hotspots region of interest can be replaced by the nanoantenna trapped nanoparticles where the OEi method would be used to switch on and off optimised traps[24,19] or even extended to selective addressing arrays of spatial biosensors.

Methods

Experimental set-up. The basic set-up used is shown in Fig. 7. A Ti:Sapphire laser (3900 S, Spectra-Physics, P_{max} = 1 W) beam is expanded to fill the aperture of the spatial light modulator, SLM (Hamamatsu LCOS-SLM X10468, resolution = 600 × 800 pixels, pixel size = 20 × 20 μm^2, refresh rate = 60 Hz) and then phase-modulated in the first order configuration[25]. The phase-modulated beam is coupled into a microscope objective (100×, Oil UPlanFL N, Olympus, NA = 1.3) and illuminates the sample consisting of gold nanostructures. The backscattered light is imaged onto a CCD camera (Basler pilot piA640-210gm, 648 × 488 pixels resolution, 7.4 μm^2 pixel size). To obtain bright-field images of the sample, it is illuminated from above by a light emitting diode.

In the case of the fiber illumination, the first diffraction order of the SLM is coupled into the multimode fibre (Thorlabs M31L05) with a NA of 0.27, and core and cladding diameters of 63 and 125 μm respectively. A telescope system consisting of 200- and 25-mm lenses ensures a light coupling efficiency of 73%. The fibre output is collimated using an 8-mm aspherical lens and is merged with the optical pathway intersecting between the folding mirror (M) and the lens (L) right after the SLM as depicted in Fig. 7.

Fabrication. As test objects to demonstrate the optical confinement and control we used periodic patterns of gold nano elements fabricated by electron beam lithography[26]. The samples were fabricated on 160 μm thick glass substrates. After thorough surface cleaning in acetone and ipa, we deposited 40 nm of Au using an electron beam evaporator at a rate of less than 0.3 nm/min, to grant a high quality metal film. We then spun a 90 nm thin layer of SU8, an epoxy based negative resist from Microchem, and wrote the desired patterns with a modified LEO/RAITH electron beam system, using an acceleration voltage of 30 KV and an irradiation dose of 10 $\mu C/cm^2$. A post exposure bake of 2 min at 100°C ensured completion of the resist cross-linking. The samples were developed in ethyl lactate for 45 s, in a low intensity ultrasonic bath. The nanofeatures were then transferred onto the Au film with a 6 min long reactive ion etching step in Argon with a forward bias of 330 V at 20 W, followed by a 2 min long gentle O2-based etch, to remove the left over resist. In particular, the utilised structures were arrays of nanoantennas and nanopads. Two

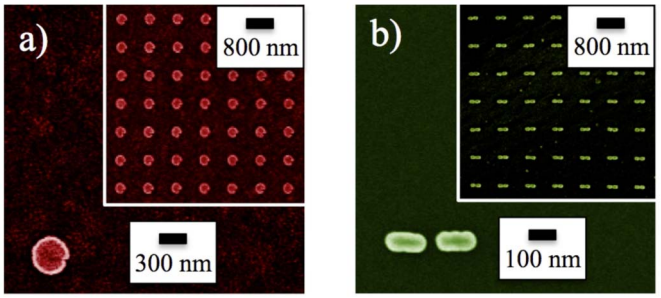

Figure 8 | SEM image of an array of (a) 300 nm nanopads spaced with a period of 800 nm and (b) 300 nm nanoantennas spaced with a period of 800 nm.

Scanning Electron Microscope (SEM) viewgraphs of typical samples are shown in Fig. 8.

Experimental method. To validate our approach, we measure the scattered field from a nanoantenna array device under coherent illumination. From the array of gold-antennas, an area consisting of n × n elements is selected. This area is homogeneously illuminated using an expanded laser beam, which serves as reference wave (E_{ref}). This reference beam is interfered with the probe fields E_j. Initially, n × n different regions of interest R_i are selected, one on top of each nanoantenna. To improve on signal to noise ratio we define a region of interest of 11 × 11 pixel^2 centred on the nano antenna.

The probe field profiles are chosen such as to optimally cover the optical degrees of freedom of a perfect non-aberated setup. We therefore numerically predetermined a set of illumination OEi of our setup (in this case N = 164). These theoretical OEi are used in our experiment as probe fields and are orthogonal in the area that accommodates the n × n nanoantennas. The next step is to experimentally measure the relative amplitude and phase of the probe fields. The probing procedure consists in displaying the superposition between the reference beam and each of the probe beams. These amplitudes and phases are then used to generate the intensity matrix operator equation 3 in the supplementary information that is subsequently used to determine the experimental optical eigenmodes.

1. Quidant, R., Petrov, D. & Badenes, G. Radiation forces on a Rayleigh dielectric sphere in a patterned optical near-field. *Opt. Lett.* **30**, 1009 (2005).
2. Righini, M., Zelenina, A. S., Girard, C. & Quidant, R. Parallel and selective trapping in a patterned plasmonic landscape. *Nat. Phys.* **3**, 477 (2007).
3. Juan, M. L., Righini, M. & Quidant, R. Plasmon nano-optical tweezers. *Nat. Photon.* **5**, 349 (2011).
4. Ploschner, M., Mazilu, M., Krauss, T. F. & Dholakia, K. Optical forces near a nanoantenna. *J. Nanophotonics* **4**, 041570 (2010).
5. Anker, J. N. *et al.* Biosensing with plasmonic nanosensors. *Nat. Mater.* **7**, 442 (2008).
6. Wang, S. *et al.* Subcellular resolution mapping of endogenous cytokine secretion by nano-plasmonic-resonator sensor array. *Nano Lett.* **11**, 3431–3434 (2011).
7. Ahmed, A. & Gordon, R. Single molecule directivity enhanced raman scattering using nanoantennas. *Nano Lett.* **12**, 2625–2630 (2012).
8. Aouani, H. *et al.* Ultrasensitive Broadband Probing of Molecular Vibrational Modes with Multifrequency Optical Antennas. *ACS Nano* **7**, 669–675 (2013).
9. Stockman, M., Faleev, S. & Bergman, D. Coherent control of femtosecond energy localization in nanosystems. *Phys. Rev. Lett.* **88**, 0674402 (2002).
10. Kubo, A. *et al.* Femtosecond imaging of surface plasmon dynamics in a nanostructured silver film. *Nano Lett.* **5**, 1123 (2005).
11. Aeschlimann, M. *et al.* Adaptive subwavelength control of nano-optical fields. *Nature* **446**, 301 (2007).
12. Volpe, G. *et al.* Controlling the optical near-field of nanoantennas with spatial phase-shaped beams. *Nano Lett.* **9**, 3608–3611 (2009).
13. Huang, S., Voronine, D., Tuchscheerer, P., Brixner, T. & Hecht, B. Deterministic spatiotemporal control of optical fields in nanoantennas and plasmonic circuits. *Phys. Rev. B* **79**, 195441 (2009).
14. Li, X. & Stockman, M. Highly efficient spatiotemporal coherent control in nanoplasmonics on a nanometer-femtosecond scale by time reversal. *Phys. Rev. B* **77**, 195109 (2008).
15. Balzarotti, F. & Stefani, F. D. Plasmonics Meets Far-Field Optical Nanoscopy. *ACS Nano* **6**, 4580–4584 (2012).
16. Gjonaj, B. *et al.* Active spatial control of plasmonic fields. *Nat. Photon.* **5**, 360–363 (2011).
17. Volpe, G., Molina-Terriza, G. & Quidant, R. Deterministic sub-wavelength control of light onfinement in nanostructures. *Phys. Rev. Lett.* **105**, 216802 (2010).
18. De Luca, A. C., Kosmeier, S., Dholakia, K. & Mazilu, M. Optical eigenmode imaging. *Phys. Rev. A* **84**, 021803(R) (2011).

19. Ploschner, M., Mazilu, M., Cizmar, T. & Dholakia, K. Numerical investigation of passive optical sorting of plasmon nanoparticles. *Opt. Express* **19** (15), 13922–13933 (2011).
20. Kosmeier, S., Mazilu, M., Baumgartl, J. & Dholakia, K. Enhanced two-point resolution using optical eigenmode optimized pupil functions. *J. Opt.* **13** (10), 105707 (2011).
21. Baumgartl, J. *et al.* Far field subwavelength focusing using optical eigenmodes. *Appl. Phys. Lett.* **98**, 181109 (2011).
22. Piestun, R. & Miller, D. A. B. Electromagnetic degrees of freedom of an optical system. *J. Opt. Soc. Am. A* **17**, 892 (2000).
23. Mazilu, M., Baumgartl, J., Kosmeier, S. & Dholakia, K. Optical Eigenmodes; exploiting the quadratic nature of the energy flux and of scattering interactions. *Opt. Express* **19**, 933 (2011).
24. Ploschner, M., Cizmar, T., Mazilu, M., Di Falco, A. & Dholakia, K. Bidirectional Optical Sorting of Gold Nanoparticles. *Nano Lett.* **12**, 1923–1927 (2012).
25. Di Leonardo, R., Ianni, F. & Ruocco, G. Computer generation of optimal holograms for optical trap arrays. *Opt. Express* **15** (4), 1913–1922 (2007).
26. Di Falco, A., Ploschner, M. & Krauss, T. F. Flexible metamaterials at visible wavelengths. *New J. Phys.* **12**, 113006 (2010).

Acknowledgements

Physical Sciences Research Council for funding (EP/J01771X/1 and EP/F040644/1), ACDL is supported by an AIRC Start-up Grant 11454, ADF is supported by an EPSRC Career Acceleration Fellowship (EP/I004602/1) and KD is a Royal Society-Wolfson Merit Award Holder. Caroline Thomson is acknowledged for setting up the Ti:Sapphire laser.

Author contributions

K.D. and M.M. developed and planned the project. M.M. performed the optical eigenmode theory, modelling and algorithm design. A.C.D.L. and S.Z. designed the optical set-up and A.C.D.L., S.Z. and S.K. built it. S.K., A.C.D.L., M.M. and S.Z. performed the experimental work and data analysis. A.D.F. designed, fabricated and characterised the nanostructures. All authors contributed to the writing of the paper.

Additional information

Supplementary information accompanies this paper at http://www.nature.com/scientificreports

Competing financial interests: The authors declare no competing financial interests.

How to cite this article: Kosmeier, S. *et al.* Coherent control of plasmonic nanoantennas using optical eigenmodes. *Sci. Rep.* **3**, 1808; DOI:10.1038/srep01808 (2013).